

A model-free temperature-dependent conformational study of *n*-pentane in nematic liquid crystals

E. Elliott Burnell,^{1,a)} Adrian C. J. Weber,^{2,b)} Ronald Y. Dong,^{3,c)} W. Leo Meerts,^{4,5,d)} and Cornelis A. de Lange^{5,e)}

¹Chemistry Department, University of British Columbia, 2036 Main Mall, Vancouver, British Columbia V6T 1Z1, Canada

²Chemistry Department, Brandon University, 270-18th Street, Brandon, Manitoba R7A 6A9, Canada

³Department of Physics and Astronomy, University of British Columbia, 6224 Agricultural Road, Vancouver, British Columbia V6T 1Z1, Canada

⁴Radboud University, Institute for Molecules and Materials, Heyendaalseweg 135, NL-6525 AJ Nijmegen, The Netherlands

⁵Laser Centre, Vrije Universiteit, De Boelelaan 1081, 1081 HV Amsterdam, The Netherlands

(Received 26 September 2014; accepted 4 December 2014; published online 14 January 2015; publisher error corrected 21 January 2015)

The proton NMR spectra of *n*-pentane orientationally ordered in two nematic liquid-crystal solvents are studied over a wide temperature range and analysed using covariance matrix adaptation evolutionary strategy. Since alkanes possess small electrostatic moments, their anisotropic intermolecular interactions are dominated by short-range size-and-shape effects. As we assumed for *n*-butane, the anisotropic energy parameters of each *n*-pentane conformer are taken to be proportional to those of ethane and propane, independent of temperature. The observed temperature dependence of the *n*-pentane dipolar couplings allows a model-free separation between conformer degrees of order and conformer probabilities, which cannot be achieved at a single temperature. In this way for *n*-pentane 13 anisotropic energy parameters (two for *trans trans*, *tt*, five for *trans gauche*, *tg*, and three for each of *gauche*₊ *gauche*₊, *pp*, and *gauche*₊ *gauche*₋, *pm*), the isotropic *trans-gauche* energy difference E_{tg} and its temperature coefficient E'_{tg} are obtained. The value obtained for the extra energy associated with the proximity of the two methyl groups in the *gauche*₊ *gauche*₋ conformers (the pentane effect) is sensitive to minute details of other assumptions and is thus fixed in the calculations. Conformer populations are affected by the environment. In particular, anisotropic interactions increase the *trans* probability in the ordered phase. © 2015 AIP Publishing LLC. [<http://dx.doi.org/10.1063/1.4904822>]

I. INTRODUCTION

The existence of multiple conformers plays an important role in the physical properties of a host of materials and, especially, in orientationally ordered systems such as liquid crystals, biological membranes, and polymers. The conformer populations are affected by intramolecular interactions and by isotropic and anisotropic interactions with the medium. In this regard, *n*-pentane is an interesting candidate for investigation, mainly because it is the shortest hydrocarbon in which a conformer exists that has low probability because of steric overlap of the chain ends.¹

Nuclear magnetic resonance (NMR) of solutes dissolved in liquid-crystal solvents is an invaluable tool for obtaining detailed information about various anisotropic interactions that in the isotropic liquid are averaged to zero. The ¹H NMR spectrum of a solute in a nematic phase is usually completely dominated by the anisotropic direct dipolar couplings. For rigid solutes, these dipolar couplings are directly related to the solute geometry and solute orientational order.

An interesting and rather common situation arises with molecules (such as *n*-pentane) that undergo conformational change that takes place much faster than the NMR time scale. The NMR spectra observed in this case are an average over all conformations, and the observed dipolar couplings in a uniaxial phase involve products of conformer probabilities and order parameters of conformers (see Sec. III for details). A key issue in NMR liquid-crystal spectroscopy is how to describe the average degree of orientational order of such a molecule that undergoes interchange among several symmetry-unrelated conformations. Here, we mean that the exchange rate among conformers is fast but normally still slow in comparison with conformer reorientational rates. Unfortunately, attempts to assume an average molecule, which then would possess a single set of at most five orientational order parameters, have been shown to be fallacious.² It is now generally accepted that every conformation requires its own set of at most five order parameters.

For a molecule with a significant number of conformations, the number of *a priori* unknown order parameters therefore can be quite large. This presents a serious bottleneck for the present case, i.e., the spectral analysis of the very complex spectra of *n*-pentane dissolved in several nematic phases. A similar situation applies to the ¹H NMR spectra of liquid-crystal molecules themselves.

a)Electronic mail: elliott.burnell@ubc.ca

b)Electronic mail: webera@brandonu.ca

c)Electronic mail: rondong@phas.ubc.ca

d)Electronic mail: leo.meerts@science.ru.nl. URL: <http://www.leomeerts.nl>

e)Electronic mail: c.a.de.lange@vu.nl. URL: <http://www.cadelange.nl>

Another challenging issue in the NMR spectroscopy of solutes in nematic phases concerns the orientation mechanisms that cause average orientational order. For small solute concentrations, the interaction between solute and solvent molecules dominates. It is not obvious beforehand what mechanisms are important in general. There now exists broad agreement that there are two mechanisms that play a crucial role. The first is a short-range mechanism that only depends on the size and shape of the solute molecule. The second is generally believed to be the interaction between the solute electric quadrupole moment and the solvent nonzero average electric field gradient.^{3,4}

In the discussion on orientational mechanisms, there are two cases that deserve special attention. One is the case of mixtures of certain nematic phases that happen to possess a zero average electric field gradient. For such “*magic mixtures*,”³ only the size-and-shape mechanism remains. The second case concerns solutes with small electrostatic moments such as molecular quadrupole moments, the so-called “*magic solutes*.”⁵ The alkanes are a case in point. For this class of solutes, the orientational order is predominantly governed by the size-and-shape mechanism. The size-and-shape interaction can be described adequately by relatively simple phenomenological models. In circumstances where the size-and-shape mechanism dominates, using these models, the degree of orientational order can be predicted at approximately the 10% level.³ Every laboratory appears to have its own favorite model.^{3,6-18} In practice, the predictions of the different models show a large degree of consistency. An earlier analysis of the NMR spectrum of orientationally ordered *n*-pentane utilized the fact that it is a magic solute and that size-and-shape models could provide a starting point for the spectral analysis.¹⁹ In a later study,²⁰ molecular dynamics (MD) simulations were employed to successfully predict spectra of *n*-pentane in the nematic liquid crystal 5CB (4-*n*-pentyl-4'-cyanobiphenyl). In a recent study on biphenyl in 5CB and 8CB, MD simulations gave good agreement with experimental dipolar couplings, and the biphenyl was found in the simulations to be rather uniformly distributed in the smectic phase of 8CB.²¹

With the direct dipolar couplings between every pair of nuclei dominating the NMR spectra of solutes in liquid-crystalline solvents, the complexity of the spectra increases very rapidly with the number of magnetic nuclei in the solute. For solutes with eight or more nuclear spins and low symmetry, the spectral analysis may become difficult to achieve. Over many years, different approaches have been attempted with varying degrees of success. Recently, we have introduced a highly powerful approach to the spectral analysis of highly complex NMR spectra based on Genetic Algorithms (GAs) or related Evolutionary Strategies (ESs). These methods have given a completely new impetus to an old field of research. The history of spectral analysis in NMR and the application of these new strategies have been summarized in a recent review article.²²

The study of conformational change dates from a long time back, but especially in the liquid phase, the importance and role of the surrounding solvent are difficult to quantify. One can approach this problem by using the dihedral-angle dependence of the J couplings in isotropic media.^{23,24} How-

ever, the authors of Ref. 24 state that their rather complex analysis is not able to transform the coupling constant information to accurate conformational energetics of the alkanes. Because of the recent advances in solving highly complex NMR spectra of solutes in anisotropic environments, we now have a new tool at our disposal for the study of conformational change in the liquid phase. Here, we investigate the use of the highly sensitive and accurate information contained in dipolar couplings.

When it comes to studying solutes that show conformational change on the NMR time scale, the *n*-alkanes provide a benchmark example. Methane, ethane, and propane exist in one conformation only, provided we neglect methyl rotation. Assuming a simple Rotational Isomeric State (RIS) model,¹ 120° rotations around every CC-bond qualitatively define the possible conformations. *n*-Butane is the first molecule in the series that undergoes conformational change, with $3^1 = 3$ conformations, 2 of which are symmetry-unrelated. *n*-Pentane possesses $3^2 = 9$ conformations, 4 of which are symmetry-unrelated. *n*-Hexane shows $3^3 = 27$ conformations, 10 of which are symmetry-unrelated. Clearly, the conformational problem increases rapidly with *n*-alkane size.

As will be discussed in Sec. III, the conformational probability p^n and the average degree of orientational order S_{kl}^n of each conformation n only occur as products that cannot be separated in a single experiment. This poses a significant problem because both the orientational order and conformer probability are parameters which we wish to extract from the experimental results. Historically, interpretation of the results usually relied on some model or theory for the anisotropic intermolecular interactions, hence providing model values for the orientational order.

With our ESs, we can now perform studies of solutes like *n*-butane and *n*-pentane in different nematic phases over a wide temperature range. As we have shown in the case of *n*-butane in a nematic environment²⁵ and in liquid crystals that exhibit both nematic and smectic A phases,²⁶ this leads to additional information that enables us to separate p^n and S_{kl}^n . The analysis depends on the observation that the anisotropic energy parameters that describe the orientational ordering scale from ethane to propane and, assuming that this scaling also applies to *n*-butane, have expedited analysis of the dipolar couplings that were obtained from the NMR spectra. For the first time we obtained novel experimental data about conformational change of *n*-butane in a liquid environment. In the present paper, we extend these ideas and carry out a study on the much more challenging solute *n*-pentane in two nematic solvents.

II. EXPERIMENTAL

The solutes *n*-pentane and 1,3,5-trichlorobenzene (abbreviated tcb and added to provide an orientational and chemical shift reference) were codissolved to 5 and 0.5 mol. % in the liquid-crystal mixture Merck ZLI-1132 (1132). After this sample was sealed and thoroughly mixed in the isotropic phase, it was placed into a Bruker Avance 400 MHz NMR spectrometer magnet. With the temperature controlled by the Bruker air-flow system, a total of 16 ¹H NMR spectra were acquired every 5° from 258.5 to 333.5 K. To extract spectral parameters with

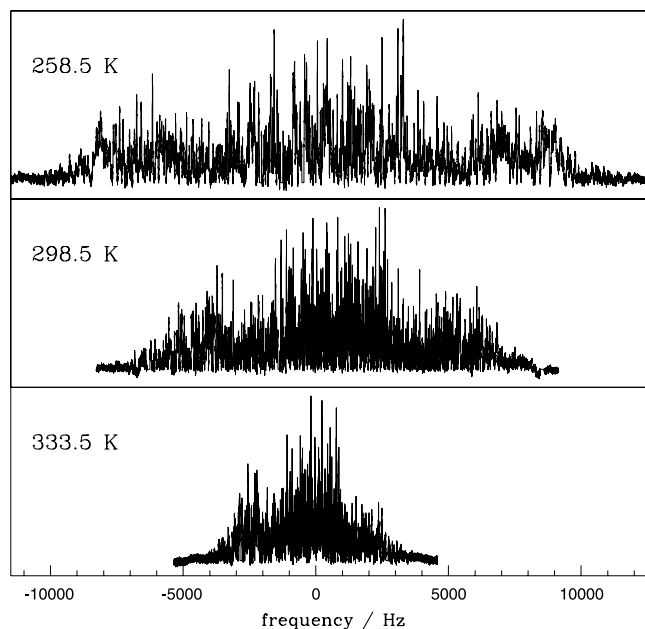


FIG. 1. Experimental spectra (80 scans) of *n*-pentane in 1132 spanning the nematic temperature range after cubic-base spline liquid-crystal background removal using about 150 points. The digital resolution is 0.6438 Hz, the line broadening is 0.1 Hz, and the signal to noise ratio is 110.

ESs, a cubic-base spline is performed to remove the background liquid-crystal signal from spectra (since the algorithm iterates on both frequency and intensity) as can be seen for three different temperatures spanning the nematic temperature range of 1132 in Figure 1. We also include in the analysis spectral parameters obtained previously²⁰ from six spectra of *n*-pentane as solute in the nematic phase of 5CB. The spectra were taken in 5° steps from 273.5 to 298.5 K. In addition, we make extensive use of the results of Ref. 27 for the solutes ethane and propane in the same liquid-crystal solvents that span essentially the same temperature ranges.

In order to obtain the spectral parameters defining the anisotropic spectra with a covariance matrix adaptation evolutionary strategy (CMA-ES), one has to first choose reasonable upper and lower limits for each parameter which defines the search space. A complete set of spectral parameters is called a chromosome and a population of these is initially spread out randomly across the search space. To evaluate the goodness of each member of the population, a fitness function needs to be defined

$$F_{fg} = \frac{(f \cdot g)}{\|f\| \|g\|}, \quad (1)$$

where \mathbf{f} and \mathbf{g} are the vector representations of the experimental and calculated spectra, and $(f \cdot g)$ is the inner product between f and g . In the experimental spectrum f , the digital resolution is always taken to be much smaller than the actual line width. This spectrum that, thus, contains line-width information implicitly is used, and the overlap with the calculated spectrum g is computed in every iteration. Here, each calculated spectral line is convoluted with a line-shape function, generally a Lorentzian with a line width estimated from the experimental spectrum. Since $(f \cdot g)$ is an inner product, it is maximal if f and g are identical. Hence, F_{fg} is a measure of

the extent to which a calculated spectrum overlaps with the experimental one which is maximum at the global minimum of the error surface where the solution is obtained.^{22,28,29} Size-and-shape models were used to provide search limits for the *n*-pentane dipolar couplings at 298.5 K in 1132 which allowed the CMA-ES to extract the fitted parameters.¹⁹ To obtain spectral parameters at an adjacent temperature, one simply uses the previous temperature values as one of the limits (depending on whether one has gone up or down in temperature). The other limit is set so as to have a search range of about 10% of the first limit. For smaller dipolar couplings, a range of ± 25 Hz was used, using an educated guess based on the value obtained at the adjacent temperature.

GAUSSIAN 09³⁰ (G09 for short) was used to calculate the gas-phase structures of the major conformers of *n*-pentane. Möller-Plesset second-order (MP2) perturbation theory³¹ was employed using Dunning's cc-pvdz basis set.³² The two internal rotational degrees of freedom, parametrized by the CCC dihedral angles ϕ_1 (about the C₂-C₃ bond) and ϕ_2 (about the C₃-C₄ bond), give rise to the four independent conformers displayed in Fig. 2. In the RIS approximation,¹ only these four structures are assumed to contribute to the conformational statistics, namely, the singly degenerate *trans trans* (tt), the four-fold degenerate *trans gauche* (tg), the two fold degenerate *gauche₊ gauche₊* (*g₊g₊* or pp), and the two-fold degenerate *gauche₊ gauche₋* (*g₊g₋* or pm). The pm turns out to have negligible probability because of the steric hindrance between methyl groups, known as the “pentane effect.”³³

Another way of treating the *n*-pentane conformational problem is by using a continuous intramolecular potential, $U_{int,n}^{iso}(\phi_1, \phi_2)$; this treatment (using continuous probability distributions) was recently used in NMR studies on *n*-butane.^{25,26,34,35} To do this for *n*-pentane, the internal energy was calculated in 15° increments of ϕ_1 and ϕ_2 while keeping all other structural parameters fixed to those of the major conformer that exists at the bottom of the local (or global in the case of tt) energy well (see Figure 3 for potential energy plotted as a function of ϕ_1 and ϕ_2). These energy wells, calculated for the *n*-pentane molecule isolated in the gas phase, are affected by the environment in the anisotropic liquid phase in which the solute is dissolved. Here, we assume that the

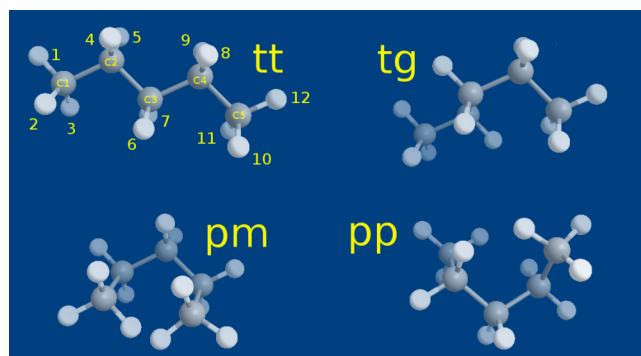


FIG. 2. The *n*-pentane conformers: tt = *trans trans*, tg = *trans gauche*, pm = *gauche₊ gauche₋*, and pp = *gauche₊ gauche₊*. Dihedral angle ϕ_1 (ϕ_2) is the extent of rotation about the C₂-C₃ (C₃-C₄) bond of conformer tt. The pm *z* axis lies along the C₁-C₅ direction of conformer tt and is close to that direction in tg and pp.

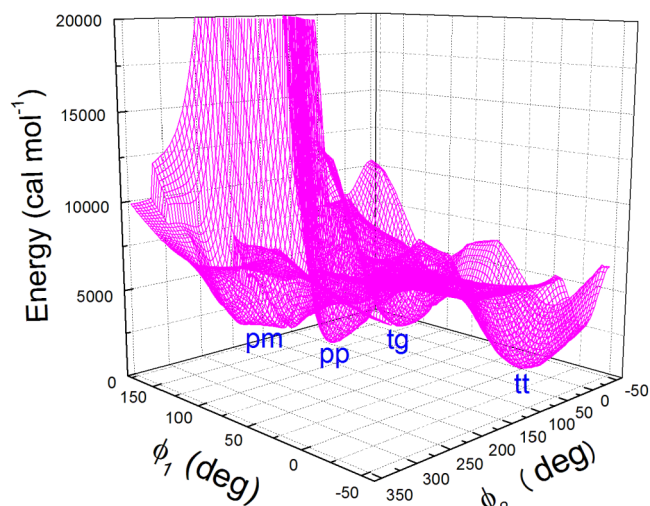


FIG. 3. The gas-phase intramolecular potential $U_{int,n}^{iso}(\phi_1, \phi_2)$ of n -pentane calculated with G09.

relative energy minima (but not the shape) of these wells will be influenced by the condensed-phase medium. Thus, the gas-phase conformational probability distributions (see Figure 4) will be affected by the anisotropic liquid environment, and fitting the observed dipolar couplings (*vide infra*) could shed light on the extent that these are modified.

III. THEORETICAL BACKGROUND

The observed dipolar couplings for a molecule in a uniaxial phase with director oriented along the magnetic-field direction can be expressed as

$$D_{ij} = \sum_n p^n \sum_{k,l} d_{kl,ij}^n S_{kl}^n, \quad (2)$$

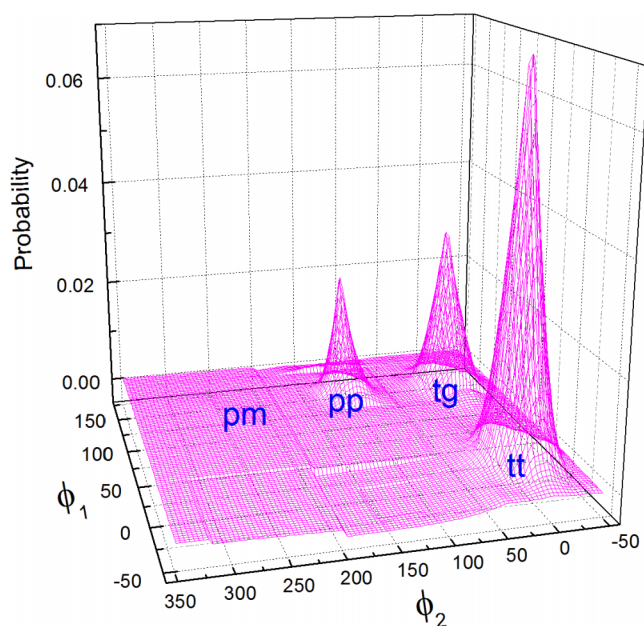


FIG. 4. The gas-phase conformational probability distribution of n -pentane calculated from the values of $U_{int,n}^{iso}(\phi_1, \phi_2)$ obtained with G09 as shown in Fig. 3.

where p^n is the probability of conformation n . The quantity $d_{kl,ij}^n$ is given by

$$d_{kl,ij}^n = -\frac{h\gamma_i\gamma_j}{4\pi^2} (\cos\theta_{ij,k}^n \cos\theta_{ij,l}^n / r_{n,ij}^3). \quad (3)$$

Here, $r_{n,ij}$ is the distance between nuclei i and j in conformation n , with $\cos\theta_{ij,k}^n$ the cosine of the angle between the ij direction in the molecule in conformation n with k a conformer-fixed axis, and γ_i is the gyromagnetic ratio of nucleus i . The Saupe order parameters for each conformation n are

$$S_{kl}^n = \left\langle \frac{3}{2} \cos\theta_{k,Z}^n \cos\theta_{l,Z}^n - \frac{1}{2} \delta_{kl} \right\rangle, \quad (4)$$

where $\cos\theta_{k,Z}^n$ is the cosine of the angle between the molecular k direction in conformation n and the space-fixed Z direction defined by the liquid-crystal director. The angle brackets indicate an ensemble average. There is a maximum of five independent second-rank order parameters for every conformation, and molecular symmetry can reduce this number. For n -pentane interchange among all possible conformers is fast and involves changes in the dihedral angles ϕ_1 and ϕ_2 . For interchange among rigid conformers (the RIS model), the observed NMR spectrum involves an average over all conformers as well as over all external conformer reorientational motions. The dipolar couplings are then given by Eq. (2).

We shall also explore the more realistic model (here called the “continuous” model) for the hydrocarbon, in which we allow for librational motions of the dihedral angles about the conformer energy well minima. The time-averaged dipolar coupling between nuclei i and j (that is obtained from analysis of the NMR spectrum) of Eq. (2) can then be written

$$D_{ij} = -\frac{h\gamma_i\gamma_j}{4\pi^2} \sum_n S_{kl}^n \sum_{\phi_1} \sum_{\phi_2} p^n(\phi_1, \phi_2) \times \left\langle \frac{1}{r_{n,ij}^3(\phi_1, \phi_2)} \cos\theta_{ij,k}^n(\phi_1, \phi_2) \cos\theta_{ij,l}^n(\phi_1, \phi_2) \right\rangle, \quad (5)$$

where the sums over ϕ_1 and ϕ_2 (restricted to be within a particular conformer well) could be written as integrals, and it is assumed that the order parameter is constant for such librations in a given conformer. An important question here involves the choice of the k and l axes and of how to define them as a function of librational motion. For such rapid internal motions (in fact for vibrations in general), one wishes to separate as much as possible the internal motion from the reorientation of the molecule as a whole. The so-called Eckart axes are the best way to do this separation (see Wilson, Decius and Cross³⁶). Still, the way in which these axes are defined is somewhat elusive. However, in many cases, the principal moment of inertia (pmi) axes provide a reasonable approximation to the Eckart axes,³⁶ and here, we use the pmi axes to carry out the separation. Hence, during a libration about a C–C bond in a given conformer, we assume that the order parameters S_{kl}^n (where k and l are pmi axes) are invariant to the librational motion. Note that the pmi axes are not necessarily the principal order axes (poa), and hence, S_{kl}^n may have off-diagonal elements.

Except for rotations about C–C bonds that are at the root of conformer changes, our treatment neglects non-rigid effects such as molecular vibrations^{37–39} and interactions between

these vibrations and molecular reorientations.^{40–42} Both non-rigid effects have been shown to make significant contributions to dipolar couplings. For example, the splittings observed in the ¹H NMR spectrum of methane as solute in nematic solvents⁴³ are a dramatic example of the effect of vibration-reorientation interaction.⁴⁰ The importance of this interaction and the difficulties involved in estimating this effect, in general, have been explored with spectra of solutes in several nematic solvents with the solutes azulene and biphenylene as examples.⁴⁴ In general, while dipolar couplings are extracted from the experimental spectra to great precision, it must be recognized that the neglected non-rigid effects essentially add a substantial uncertainty. This uncertainty is of little consequence to the present study which involves many other assumptions and thus is not expected to fit the dipolar couplings to great accuracy.

Equation (5) with the above set of approximations worked well for a recent investigation of *n*-butane which involved a

single dihedral angle where the sum over ϕ was carried out in 5° steps over all possible dihedral angles.²⁵ With *n*-pentane, we choose to sum over each dihedral angle between -45° and +45° (from the well minimum) in 7 steps of 15° each. For the four independent wells, this involves $4 \times 7 \times 7 = 196$ calculations that must be performed in the minimization routine. We also include rotation of the two methyl groups in 4° steps. The result is that the minimization involving fitting of 22 spectra (16 of *n*-pentane in 1132, 6 in 5CB) simultaneously takes of order one day single-processor central processing unit time.

The interesting but elusive parameter that is of interest in the NMR investigation of orientationally ordered flexible solutes is the conformer probability, p^n . This parameter is a function of the gas-phase conformer energy, the effect of the condensed liquid-phase isotropic intermolecular interactions on the conformer energy, and the effect of the orientational order through the anisotropic intermolecular interactions. In general, the conformer probability in Eq. (5) is

$$p^n(\phi_1, \phi_2) = \frac{G^n(\phi_1, \phi_2) \exp(-U_{ext,n}^{iso}/kT) \exp(-U_{int,n}^{iso}(\phi_1, \phi_2)/kT) \int \exp(-U_n^{aniso}(\Omega)/kT) d\Omega}{\sum_n \sum_{\phi_1} \sum_{\phi_2} G^n(\phi_1, \phi_2) \exp(-U_{ext,n}^{iso}/kT) \exp(-U_{int,n}^{iso}(\phi_1, \phi_2)/kT) \int \exp(-U_n^{aniso}(\Omega)/kT) d\Omega}, \quad (6)$$

where $G^n(\phi_1, \phi_2) = \sqrt{I_{xx}^n I_{yy}^n I_{zz}^n}$ is a rotational kinetic energy factor which is dependent on the principal values of the moment of inertia tensor for each conformer,¹³ $U_{ext,n}^{iso}$ is the isotropic component of the intermolecular potential between the solute and the solvent, and $U_{int,n}^{iso}(\phi_1, \phi_2)$ is the intramolecular contribution to the conformer energy (i.e., the gas-phase value). $U_n^{aniso}(\Omega)$ is the anisotropic component of the intermolecular potential between the solute and the solvent and for conformer *n* is

$$U_n^{aniso}(\Omega) = - \sum_{k=xyz} \sum_{l=xyz} \frac{3}{4} G_{ZZ}(\text{LC}) \beta_{kl}(n) \times \cos(\theta_{k,Z}^n) \cos(\theta_{l,Z}^n). \quad (7)$$

Here, β is the anisotropic part of some solute electronic property and $G_{ZZ}(\text{LC})$ is the axially symmetric liquid-crystal field of a uniaxial medium.

The conformer orientational order parameters of Eq. (4) only depend on the anisotropic part of the intermolecular potential and are given by

$$S_{kl}^n = \frac{\int (\frac{3}{2} \cos(\theta_{k,Z}^n) \cos(\theta_{l,Z}^n) - \frac{1}{2} \delta_{kl}) \exp(-U_n^{aniso}(\Omega)/kT) d\Omega}{\int \exp(-U_n^{aniso}(\Omega)/kT) d\Omega}. \quad (8)$$

In addition to their dependence on the anisotropic intermolecular potential, the conformer probabilities also depend on the intra- and extra-molecular isotropic energies. For the RIS model, the various contributions are included in Eq. (6) when ϕ_1 and ϕ_2 are both set to the values that correspond to a particular (relative) conformer energy minimum.

IV. RESULTS AND DISCUSSION

Sixteen sets of dipolar couplings measured for *n*-pentane in 1132 at temperatures between 258.5 and 333.5 K and obtained from CMA-ES spectral fitting are reported in Table I. We also include in the analysis six sets of dipolar couplings measured for *n*-pentane in the nematic liquid crystal 5CB at temperatures between 273.5 and 298.5 K.²⁰ Unfortunately, as indicated earlier, only the product $S^n \times p^n$ in Eq. (2) can be obtained from the dipolar couplings. Hence, S^n and p^n cannot be separated at a single temperature without invoking models either for S^n or for p^n . In this paper, we employ the temperature dependence of the conformer probabilities p^n (or rather of the anisotropic intermolecular potential) to allow separation. In addition, we use the observation that the ratios of propane to ethane energy parameters are essentially constant with changing temperature.²⁷ Hence, as we did for *n*-butane, we assume that the anisotropic energy parameters of each *n*-pentane conformer are proportional to that for ethane. The important point is that we do not employ any model for the anisotropic interactions between solute and liquid crystal.

The *tt* conformer has C_{2v} symmetry and requires two order parameters, *pm* has C_{1h} symmetry with three order parameters, *pp* has C_2 symmetry with three order parameters, and *tg* has no symmetry (C_1) with five order parameters. Hence, the orientational order of the four independent conformers of *n*-pentane involves 13 independent order parameters and in turn these require specification of 13 independent $G_{ZZ}(\text{LC})\beta_{kl}(n)$ energy parameters.

To proceed, we use Eq. (7) and assume that all the conformers of *n*-pentane, as well as those of *n*-butane, ethane, and propane, experience a precisely identical axially symmetric liquid-crystal field $G_{ZZ}(\text{LC})$ which varies with liquid-crystal solvent and temperature. The temperature dependence of the

TABLE I. Sixteen sets of dipolar couplings of *n*-pentane and tcb in 1132 as a function of temperature. The error in the couplings is of order 0.1 Hz.

T / K	D_{tcb}	$D_{1,2}$	$D_{1,4}$	$D_{1,6}$	$D_{1,8}$	$D_{1,10}$	$D_{4,5}$	$D_{4,6}$	$D_{4,7}$	$D_{4,8}$	$D_{4,9}$	$D_{6,7}$
258.5	267.17	1646.91	-303.04	-1014.09	-482.55	-248.58	3683.47	29.51	127.62	-1592.07	-925.19	3846.41
263.5	262.14	1582.10	-291.12	-972.28	-470.20	-241.35	3544.46	21.93	119.13	-1512.91	-893.70	3706.20
268.5	256.98	1518.48	-279.05	-931.31	-457.39	-234.01	3406.96	14.14	111.63	-1436.54	-862.49	3566.09
273.5	251.26	1453.23	-266.79	-889.52	-443.41	-226.20	3265.69	7.48	104.05	-1359.86	-830.14	3422.50
278.5	245.28	1390.96	-255.22	-849.85	-429.54	-218.63	3130.35	1.68	96.56	-1288.43	-798.31	3284.83
283.5	239.28	1331.19	-244.13	-811.83	-415.54	-211.14	3000.09	-3.16	89.73	-1221.05	-767.35	3151.61
288.5	232.85	1269.32	-232.71	-772.50	-400.43	-203.11	2864.66	-8.29	83.51	-1152.79	-734.96	3012.14
293.5	225.98	1208.73	-221.49	-734.27	-385.10	-195.01	2731.86	-12.58	77.56	-1087.44	-702.46	2875.62
298.5	218.30	1143.12	-209.46	-693.10	-367.75	-186.08	2587.79	-16.56	71.43	-1018.63	-666.86	2727.19
303.5	210.66	1081.44	-198.27	-654.54	-350.90	-177.40	2451.93	-20.00	66.21	-955.85	-632.83	2586.57
308.5	202.19	1016.58	-186.33	-614.13	-332.73	-168.01	2308.46	-22.30	60.26	-890.55	-597.10	2437.36
313.5	190.75	935.11	-171.51	-563.85	-308.60	-155.79	2127.62	-24.59	54.18	-812.09	-550.68	2249.01
318.5	179.72	861.92	-158.15	-518.83	-286.65	-144.63	1964.70	-25.96	48.72	-742.58	-509.10	2079.28
323.5	166.30	779.31	-143.05	-468.20	-261.02	-131.67	1779.58	-26.77	43.07	-665.90	-461.37	1885.35
328.5	148.85	678.25	-124.63	-406.79	-228.72	-115.38	1552.53	-26.17	36.48	-575.08	-402.76	1646.86
333.5	121.66	536.10	-98.58	-320.95	-182.01	-91.80	1230.48	-23.20	28.13	-450.97	-319.06	1307.16

13 independent $G_{ZZ}(\text{LC})\beta_{kl}(n)$ parameters is given by scaling to the $G_{ZZ}(\text{LC})\beta_{\text{ethane}}$ values where LC = 1132 or 5CB.

There are internal (to the solute) and external (between solute and liquid crystal) components to the isotropic part of the conformer potential energy that affect the conformer probabilities of Eq. (6). They both appear in a similar form in exponentials of this equation and cannot be separated with our experimental results. Hence, we must set a value for one in order to obtain information about the other. Here, we use G09 to calculate the isolated molecule (*gas-phase*) energy for each conformer used. Full geometry optimization was used to locate the four independent conformer-well minima. For librations involving values of ϕ_1 and/or ϕ_2 away from the conformer-well minima, the geometry (except for ϕ_1 and/or ϕ_2) was fixed at that for the well minimum.

As long as we assume that $U_{\text{ext},n}^{\text{iso}}$ does not depend on ϕ , but only on conformer n , we are left with three unknown energy parameters, E_{tg} , E_{pm} , and E_{pp} ; these being the difference in energy between the energetically most favorable tt and the less favorable tg, pm, and pp conformer energy wells

$$\begin{aligned} E_{\text{tg}} &= U_{\text{tg}}^{\text{iso}} - U_{\text{tt}}^{\text{iso}} = E_{\text{tg}}^{\text{int}} + E_{\text{tg}}^{\text{ext}}(T), \\ E_{\text{pm}} &= U_{\text{pm}}^{\text{iso}} - U_{\text{tt}}^{\text{iso}} = E_{\text{pm}}^{\text{int}} + E_{\text{pm}}^{\text{ext}}(T), \\ E_{\text{pp}} &= U_{\text{pp}}^{\text{iso}} - U_{\text{tt}}^{\text{iso}} = E_{\text{pp}}^{\text{int}} + E_{\text{pp}}^{\text{ext}}(T). \end{aligned} \quad (9)$$

The values we use (from the G09 calculation results shown in Fig. 3) for $E_{\text{tg}}^{\text{int}}$, $E_{\text{pm}}^{\text{int}}$, and $E_{\text{pp}}^{\text{int}}$ are 480, 3263, and 658 cal mol⁻¹, respectively.

For *n*-butane, the value of E_{tg} was found to vary with temperature.²⁵ Here, we introduce a similar temperature dependence for the *n*-pentane energy parameters. For the tg conformer, we use

$$E_{\text{tg}}^{\text{ext}}(T) = E_{\text{tg}}^{\text{ext}}(300) + E'_{\text{tg}}(T - 300\text{K}). \quad (10)$$

The temperature dependence for conformers pm and pp is discussed below.

Some dipolar couplings are much more sensitive to conformer change than others. In particular, the $\frac{1}{r_{ij}^3}$ term in D_{ij}

changes dramatically with conformer change for $ij = 46, 47, 48$, and 49 (see Fig. 2 for H-atom numbering). Hence, in the least-squares fitting, we weigh these couplings about three times more heavily than those for which geometric factors play a lesser role.

Each spectrum provides 11 independent dipolar couplings, but is characterized by 13 independent, unknown order parameters. Hence, the analysis of a single spectrum is underdetermined. It is through the temperature dependence of conformer populations that we strive to extract information. Thus, with 22 spectra, in principle we have $22 \times 11 = 242$ independent D_{ij} .

A glance at the temperature dependence of the D_{ij} ratios in Fig. 5 shows that, in fact, not all 242 couplings are truly independent. For most of the temperature range, the eleven ratios are observed to be represented by straight lines, characterized by an intercept and a slope. Sometimes some curvature in the lines is observed (for example $D_{n\text{-pentane}}(4,8)/D_{\text{ethane}}$ in Fig. 5) but this does not take away from the fact that the 242 couplings really only provide of order 22 experimental values (i.e., the slopes and intercepts of the 11 lines) that contribute independently to the results of the fitting procedure.

In the fitting, we are interested in obtaining information about parameters such as E_{tg} , E_{pm} , and E_{pp} (three parameters) and their temperature dependence (three more parameters). We also need to deal with the anisotropic intermolecular potential, and in general, there are 13 $G\beta$ energy parameters for each spectrum, one for each independent order parameter. In order to keep the problem manageable, we fix geometry parameters to values determined in the G09 calculations, including the methyl CCH angle. Note that in earlier work on *n*-pentane¹⁹ that used a geometry from Gaussian 03 using B3LYP/6-311++G**, the best fits involved a change in the methyl CCH angle of over 2°. This change was ascribed to the effects of vibration-reorientation coupling.⁴⁴ In the present *n*-pentane case where we use MP-pvdz G09 to calculate geometry, only small changes in this CCH angle are observed when it is allowed to vary. Hence, we decided to fix it to the G09 geom-

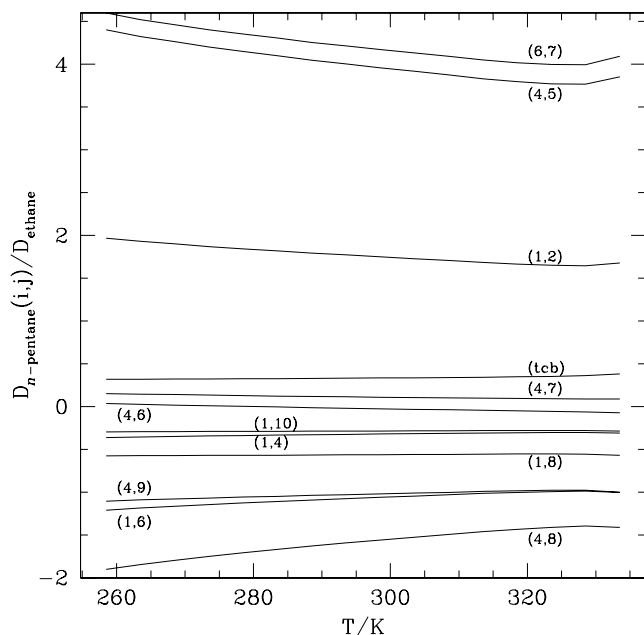


FIG. 5. $D_{ij}(n\text{-pentane})/D_{\text{ethane}}$ ratios versus T . Each ratio is labeled by (i, j) . Note, if conformer probabilities did not change with temperature (and if the orientational order of the n -pentane conformers is, as assumed, proportional to that of ethane), then the lines would be horizontal. Examination of Eq. (2) then indicates that the non-horizontal lines result from the temperature dependence of the conformer probabilities, p^n . This temperature dependence of conformer probabilities can give information about conformer energies. Note that the changes in slope for the two highest-temperature points (328.5 and 333.5 K) are due to a large uncertainty in D_{ethane} values which are obtained from an extrapolation of the ethane couplings that were only measured at lower temperatures. In the final fitting, these two higher-temperature D_{ethane} values are treated as unknowns to be fitted.

etry. These findings emphasize the importance of an accurate geometry for cases that involve different conformers. Usually, as is also the case here, the number of structural parameters far exceeds the number of observed dipolar couplings. Hence, if we want to investigate anisotropic energy parameters, we have no choice but to rely heavily on the quality of the structure calculations. This is all the more true if we wish to extract anisotropic energy parameters without invoking an *a priori* model for them.

Obviously, the parameters can be fitted to the experimental results in many different ways. The various fits that we attempted show that, when E_{pm}^{ext} or E_{pp}^{ext} is allowed to vary independently, we do not obtain sensible values as the fits yield unacceptably large probabilities for the pm or pp conformer. We know of no *a priori* choice for these parameters. In order to proceed, we make the assumption that $E_{pm}^{\text{ext}}(T)$ and $E_{pp}^{\text{ext}}(T)$ are affected by every *gauche* rotation in the solute to the same extent. Thus, we fix the values of $E_{pm}^{\text{ext}}(T)$ and $E_{pp}^{\text{ext}}(T)$ (two rotations) to twice the value of $E_{tg}^{\text{ext}}(T)$ (one rotation) as given by Eq. (10). An added bonus of this procedure is that it helps to keep the number of adjustable parameters to a minimum. The inclusion of a linear temperature dependence for all three of E_{tg} , E_{pm} , and E_{pp} gives the best fits to the experimental D_{ij} and gives the fit parameters reported in Table II. Hence, in addition to the 13 $G_{ZZ}\beta(n)$ anisotropic energy parameters for four symmetry-unrelated conformers, we adjust only the two conformational energy parameters, $E_{tg}^{\text{ext}}(300)$ and E'_{tg} of Eq. (10).

First, we do simultaneous fits to all 22 spectra (16 from 1132, 6 from 5CB) by adjusting 13 $G_{ZZ}(\text{LC})\beta_{ij}(n)$ parameters and by using the $G(\text{LC})\beta_{\text{ethane}}$ values to achieve temperature scaling. In addition to the $G\beta$ parameters, the fits also involve adjusting the energy parameters $E_{tg}^{\text{ext}}(300)$ and E'_{tg} . As mentioned above, the parameters E_{pm}^{ext} and E_{pp}^{ext} are set equal to $2E_{tg}^{\text{ext}}$. When we set $E'_{tg} = 0$, the RMS of the fit increases from 7.3 to 17 Hz (continuous potential with all 22 spectra). It must be emphasized that the most interesting result is that $E_{tg}^{\text{ext}}(300)$ and E'_{tg} are well determined, especially for fitting all 22 spectra. Particularly interesting is that the value of E'_{tg} (of order -2 cal K^{-1}) is consistent with the value found for n -butane in an earlier study.²⁵ Second, we do separate fits (shown in Table II) to the 16 spectra of n -pentane in 1132 and to the 6 spectra of n -pentane in 5CB.

In all three cases in which we attempt the fitting the problem is well posed. However, the temperature dependence assumed for the conformer relative well depths imposes correlations among parameters at different temperatures.

From the various fits, the relevant $G\beta$ second-rank tensor elements are obtained in pmi axes defined for each conformer tt, tg, pm, and pp. These tensors can be diagonalized to obtain their principal values and the poa. Since the S tensors for each conformer are directly related to the $G\beta$ tensors through Eq. (8), both the $G\beta$ and S tensors are diagonal in the same poa. The principal S values and angles between pmi and poa axes as well as both E_{tg} energy parameters are given in Table II for five different analyses. The situation with E_{pm} , E_{pp} , and their possible temperature dependences will be discussed below. Columns 2 to 4 report analyses based on the continuous model (see Eqs. (5) and (6)), while columns 5 and 6 are for the RIS model. A measure of the quality of the various fits is given by the respective RMS values.

The results of the fits to either the 5CB or 1132 set of spectra differ somewhat from the fits to all 22 spectra, especially the diagonalization angles (see Table II). When using both 1132 and 5CB spectra (fitting 11 couplings times 22 spectra), the problem appears to be well posed, despite the correlations among parameters alluded to above.

In the approach we have taken with n -butane²⁵ and now with n -pentane, we aim to work model free. For the anisotropic intermolecular potential, we parameterize the problem in terms of $G\beta$ tensor elements which depend on no specific model, other than that the interaction is second-rank, i.e., takes the form of Eq. (7). So far, the usual method of dealing with hydrocarbon-chain NMR was to use a specific model for the anisotropic intermolecular potential and then to adjust the model parameters to obtain the best fit to the observed spectral dipolar couplings. Phenomenological theories especially developed to deal with hydrocarbon chains are the chord and modified-chord models¹² in which the intermolecular potential is described with a limited number of model parameters. Each of these potentials has the conventional Maier-Saupe form.^{45,46} As an aside and in order to make a crude comparison with our model-free approach, we report a RIS fit (column 6) of the two-parameter modified chord model to our experimental results, again using the ethane $G\beta$ values in 1132 and 5CB as a function of temperature to scale the energy parameters. A simultaneous fit to all our 22 spectra obtained with the modified

TABLE II. Parameters^a obtained from the continuous-potential and RIS fits. The θ angles are the angles between the pmi and poa axes.^b

Calculation	Continuous			RIS	RIS modchord ^c	Average ^d
	5CB	1132	1132 and 5CB	1132 and 5CB	1132 and 5CB	
S_{zz}^{tt}	0.2232	0.4208	0.3595	0.3951	0.3739	0.39 ± 0.03
$(S_{xx} - S_{yy})^{tt}$	-0.1362	-0.0912	-0.0666	-0.0789	-0.0106	-0.08 ± 0.01
S_{zz}^{tg}	0.1455	0.2621	0.2528	0.2977	0.2615	0.27 ± 0.02
$(S_{xx} - S_{yy})^{tg}$	0.2051	0.0733	0.0464	0.2127	-0.0715	0.11 ± 0.09
θ_x^{tg}	4.9	14.6	45.7	10.6	2.7	24 ± 19
θ_y^{tg}	6.5	15.4	45.6	9.9	2.9	24 ± 19
θ_z^{tg}	4.7	6.2	7.0	4.6	1.1	6 ± 1
S_{zz}^{pm}	0.1429	0.1626	0.1578	0.2798	0.0947	0.20 ± 0.07
$(S_{xx} - S_{yy})^{pm}$	0.5700	0.6776	0.6547	0.5830	0.2143	0.64 ± 0.05
θ_x^{pm}	7.1	35.7	32.1	10.7	2.2	26 ± 13
S_{zz}^{pp}	-0.1085	0.0579	0.1437	-0.1166	0.1050	0.03 ± 0.13
$(S_{xx} - S_{yy})^{pp}$	0.0182	-0.2602	-0.2597	0.2376	-0.0876	-0.09 ± 0.29
θ_x^{pp}	26.4	17.6	11.6	19.6	1.0	16 ± 4
$E_{ig}^{ext}(300) / \text{cal}$	-127	-167	3	48	30	-39 ± 114
$E'_{ig} / \text{cal K}^{-1}$	-1.42	-1.75	-2.15	-1.71	-1.57	-1.87 ± 0.25
rms/Hz	2.1	6.2	7.3	9.2	24	

^aOrder parameters are for spectra at 298.5 K and (except for 5CB in column 2) are reported for spectra in 1132.

^bThe $x y z$ are the poa. For tt, in the central CH₂, x is the H-H direction, y is the HCH bisector (the C₂ axis) and z , perpendicular to the central HCH plane, is the long axis (connecting the terminal carbons). For tg, pm, and pp, the poa axes are rotated from the pmi axes by angles θ . For pm, the rotation is about the z axis, while for pp it is about the y axis. In all cases, z is the longest direction within the conformer shape. For conformers pm and pp, S_{zz} is not always the most positive order parameter: the larger variation with fit of this parameter indicates it is not well determined.

^cThe modified chord fitting values for 1132 at 298.5 K are $\bar{w}_0 = 200 \text{ cal mol}^{-1}$ and $\bar{w}_1 = 223 \text{ cal mol}^{-1}$. Values found for *n*-butane in 1132 at 298.5 K are $\bar{w}_0 = 210.5 \text{ cal mol}^{-1}$ and $\bar{w}_1 = 195.4 \text{ cal mol}^{-1}$.³⁵ The definition of these chord parameters is as given in Refs. 12 and 19.

^dThe average is over values in columns 3-5, and the error is the standard deviation of the average.

chord model shows an RMS value that is significantly worse than was achieved with our various model-free fits in Table II.

Some of the results vary a lot with the spectra chosen for the fitting. Column 7 reports the average of values in columns 3–5 selected from the results for the 1132 sample at 298.5 K, and the error is the standard deviation of this average. A small error indicates that the parameter is relatively independent of analysis details, and that the value has merit, as is the case for S_{zz}^{tt} , $(S_{xx} - S_{yy})^{tt}$, S_{zz}^{tg} , θ_z^{tg} , $E_{ig}^{ext}(300)$, and E'_{ig} . The values of θ_x^{tg} and θ_y^{tg} are not well determined, primarily because $(S_{xx} - S_{yy})^{tg}$ is in some instances small, and thus the conformer is behaving somewhat like a symmetrical cylinder for which the value would be zero and the angle undetermined.

From the fits to the 16 spectra in 1132 and the joint fits to the 22 spectra (6 from 5CB and 16 from 1132), we obtain average (over columns 3-5 of Table II) values for $E_{ig} = E_{ig}^{int} + E_{ig}^{ext}(T)$ to be in the range of $441 \pm 114 \text{ cal mol}^{-1}$ at 300 K with a temperature variation of $-1.9 \pm 0.3 \text{ cal K}^{-1} \text{ mol}^{-1}$. The value obtained for E'_{ig} is consistently in the range of $-2 \text{ cal K}^{-1} \text{ mol}^{-1}$ and very similar to that obtained for *n*-butane.²⁵ For the same calculations, the average of the conformer populations (at 298.5 K) are: tt (0.33 ± 0.03 [0.30]); tg (0.51 ± 0.01 [0.54]); pm (0.02 ± 0.01 [0.005]); and pp (0.14 ± 0.01 [0.16]) with the value for the isotropic intermolecular potential only given in square parentheses. The effect of the orientational potential is noted in the difference between conformer populations in the isotropic and the ordered phases at 298.5 K.

The conformer populations are affected both by the temperature dependence of E_{ig} and by the $k_B T$ term in the

Boltzmann factors. This temperature dependence of the population differences between ordered and isotropic phases is shown in Fig. 6 for the continuous joint fits to the 22 spectra (6 from 5CB and 16 from 1132, column 4 of Table II). From this figure, we see that conformer pm has low probability and therefore contributes little to the overall average D_{ij} values obtained from the NMR spectra. This low probability is a direct result of the high energy calculated for this conformer by G09—if we try to fit this probability, rather large values are obtained. Such large values are rejected on the basis of the pentane effect, i.e., the steric hindrance between methyl groups in this conformer. Thus, the parameters for conformer pm are not well determined. Also order parameter values for the pp conformer are unfortunately sensitive to the method of analysis, and these numbers and the associated diagonalization angles are not trustworthy.

The effect of orientational order is clearly seen in Fig. 6. For example, the probability of the tt (and to some extent the pm) conformer is increased by the orientational order and that of the tg (and to some extent the pp) conformer is decreased. The effects are greater for 1132 than for 5CB because 1132 is more ordered than is 5CB at all temperatures. These observations are an indication of the expectation that the longer tt conformer is more easily accommodated by the ordered nematic phase than is the more globular tg conformer.

Note that the pmi axes are a rough measure of molecular shape and to a first approximation we expect the poa to lie close to the pmi axes, i.e., we expect the θ values to be small as is the case for θ_z^{tg} . The results in column 6 of Table II of a fit

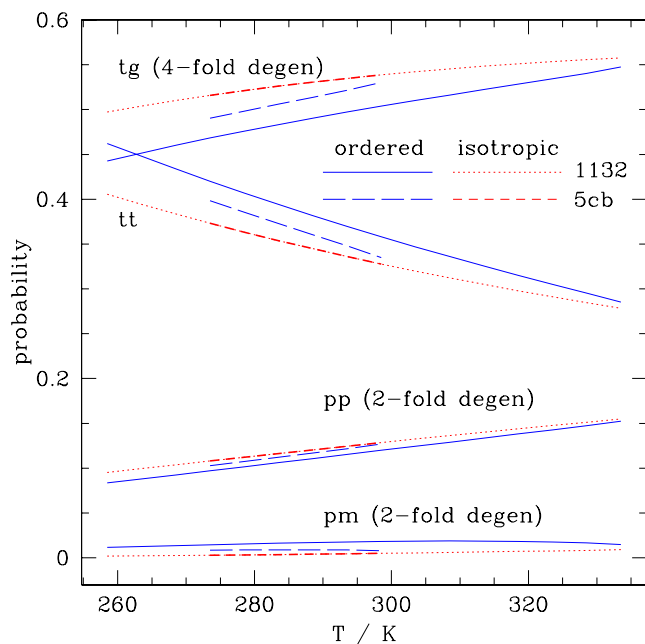


FIG. 6. p^n versus T for calculation continuous / 1132 and 5CB in Table II. The red dotted (1132) and short-dashed (5CB) lines are for the isotropic intermolecular potential, and the blue long-dashed (5CB) and solid (1132) lines include the orientational potential. Note that the isotropic contribution is identical for both liquid crystals.

to all 22 spectra using the modified chord model¹² produces, as expected, small θ diagonalization angles, i.e., the poa axes lie very close to the pmi axes for the modified chord model. Comparison of order parameters calculated by this model with those obtained without the use of a model for orientational

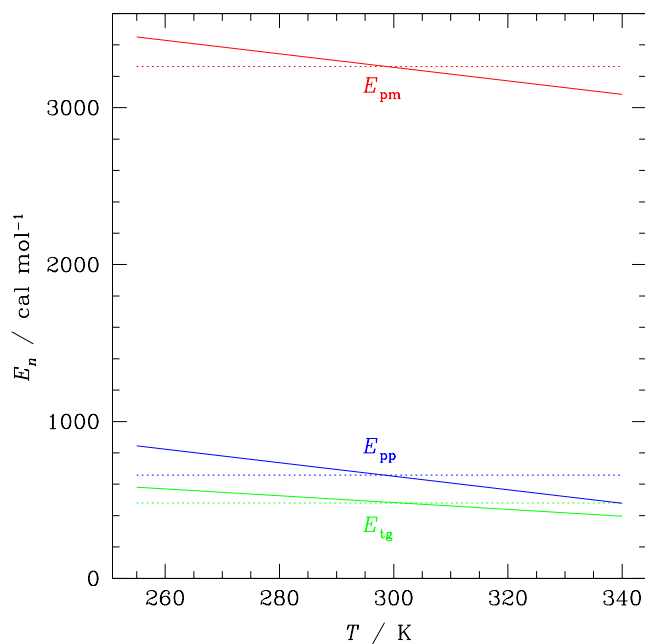


FIG. 7. Values of E_n versus T for conformers $n = \text{tg}, \text{pm},$ and pp , see Eq. (9). The horizontal dotted lines are the G09 MP2 energy values from the G09 calculations for the local potential-well minima: $E_{\text{tg}}^{\text{int}} = 480 \text{ cal mol}^{-1}$, $E_{\text{pm}}^{\text{int}} = 3263 \text{ cal mol}^{-1}$, and $E_{\text{pp}}^{\text{int}} = 658 \text{ cal mol}^{-1}$. The solid lines include the $E_n^{\text{ext}}(T)$ calculated from Eq. (10) using the $E_{\text{tg}}^{\text{ext}}(300)$ and E_n' values for the combined fitting of 5CB and 1132 results to the continuous potential in Table II. The quantities $E_{\text{pm}}^{\text{ext}}$ and $E_{\text{pp}}^{\text{ext}}$ are dealt with as explained in the text.

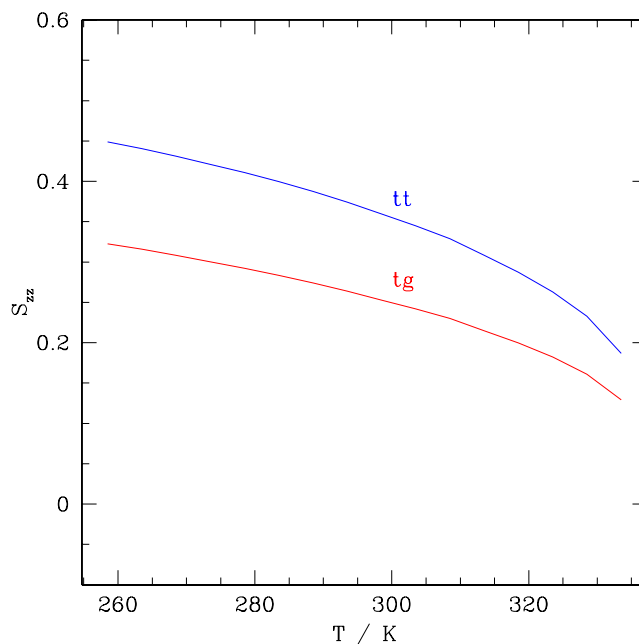


FIG. 8. Principal order parameter S_{zz} versus T of n -pentane conformers tt and tg in 1132; continuous-potential fit to both 1132 and 5CB as discussed in text.

order (columns 2-5) shows that some order parameters agree reasonably well (for example, S_{zz}^{tt} and S_{zz}^{tg}) while others show large variation.

In principle, many parameters could be adjusted in the fit to the 242 experimental dipolar couplings; but as indicated above, the temperature dependence really reduces the number of useful experimental measurements to about 22. Regardless, for many different ways of attempting to fit the results, essentially the same number for the temperature dependence $E_{\text{tg}}' \approx -2 \text{ cal K}^{-1}$ is obtained. In all cases, the intramolecular $E_{\text{tg}}^{\text{int}}$, $E_{\text{pm}}^{\text{int}}$, and $E_{\text{pp}}^{\text{int}}$ values in Eq. (9) are set to those calculated by G09. In Fig. 7, we show the resulting energy values as a function of temperature for the simultaneous fit of all 5CB and 1132 dipolar couplings using the continuous model calculation.

The most positive principal S values for conformers tt and tg are displayed in Fig. 8. In each case, the value is for the longest axis in terms of the conformer shape. The result is consistent with the expectation from size-and-shape models that the most positive order parameter should be associated with the longest conformer axis. When we examine similar plots for various other assorted fitting schemes, we always find that the values for tt are larger than for tg , and the numbers obtained are “similar” to those in the figure. This is to be expected because the “folded” nature of tg should lead to lower orientational order. Order parameter values for conformers pm and pp tend to vary a lot with calculation. For example, the value for pp is negative in some instances. The erratic behaviour for pm is not surprising because only about 1% of molecules adopt this conformer. The asymmetry in the order matrix also depends on calculation, and cannot be used reliably.

V. CONCLUSIONS

Here, we report a very accurate set of dipolar couplings obtained from the very complicated NMR spectra of n -pentane

(each spectrum consisting of roughly 20,000 transitions). These couplings have been obtained over a sufficiently large temperature range to affect the conformer populations to an appreciable extent, and they have been obtained using two different nematic liquid-crystal solvents. It is quite impressive that we are able to obtain an RMS difference between experimental and recalculated dipolar couplings for all 22 spectra combined of only about 7 Hz—a number that up to now has been considered excellent for fitting results to a single spectrum when using some model for the ordering potential. The fitting of the entire set of couplings should be used in the future for any new ideas that might arise for their interpretation.

In this paper, we have investigated the effect of condensed phases, especially anisotropic liquids, on the conformational nature of *n*-pentane. The presence of four symmetry-unrelated conformers gives rise to many unknowns. In addition, the fact that the experimental dipolar couplings all involve products of conformer probability times order matrix elements (it being impossible in a simple way to separate probability from order parameter) makes analysis particularly difficult without using some model for the orientational potential. However, here we have managed to do away with the use of any model. We have used the temperature dependence of the dipolar couplings in conjunction with energy parameters for ethane obtained in the same liquid-crystal solvent to extract information on *n*-pentane conformer energies and probabilities. An important aspect of the analysis is based on the fact that hydrocarbons are magic solutes for which the orientational potential is dominated by size-and-shape effects. This idea is reinforced by the observation that the anisotropic energy parameters for propane scale to those for ethane. In addition, the successful conformational analysis of the temperature dependence of spectra of *n*-butane in the same liquid-crystal solvents was based on this same scaling assumption.²⁵ Using this same assumption for *n*-pentane, we obtain a single value for each of 13 independent energy parameters (using the ethane energy parameters for the same liquid-crystal solvent as scaling for the other temperatures) and fit 22 spectra with a RMS of 7 Hz. This value is better than the RMS when the modified chord model is used for predicting the order parameters of the four symmetry-unrelated conformers of *n*-pentane. Furthermore, we believe that a comparison between our model-free approach and the model-dependent calculation (column 4 versus column 6 in Table II) would suggest that most of the fitted parameters are at least in qualitative agreement.

Probably, the most important result of this paper is that the temperature variation of E'_{ig} of about $-2 \text{ cal K}^{-1} \text{ mol}^{-1}$ is quite similar to the value obtained for *n*-butane.²⁵ Explanation of this effect presents a challenge for the future.

ACKNOWLEDGMENTS

E.E.B. and R.Y.D. thank the Natural Sciences and Engineering Research Council of Canada for financial support.

¹P. J. Flory, *Statistical Mechanics of Chain Molecules* (Wiley-Interscience, New York, 1969).

²E. E. Burnell and C. A. de Lange, *Chem. Phys. Lett.* **76**, 268 (1980).

³E. E. Burnell and C. A. de Lange, *Chem. Rev.* **98**, 2359 (1998).

⁴*NMR of Ordered Liquids*, edited by E. E. Burnell and C. A. de Lange (Kluwer Academic Publishers, Dordrecht, The Netherlands, 2003), ISBN 1-4020-1343-4.

⁵A. F. Terzis, C.-D. Poon, E. T. Samulski, Z. Luz, R. Poupko, H. Zimmermann, K. Müller, H. Toriumi, and D. J. Photinos, *J. Am. Chem. Soc.* **118**, 2226 (1996).

⁶J. M. Anderson, *J. Magn. Reson.* **4**, 231 (1971).

⁷J. C. Robertson, C. T. Yim, and D. F. R. Gilson, *Can. J. Chem.* **49**, 2345 (1971).

⁸J. P. Straley, *Phys. Rev. A* **10**, 1881 (1974).

⁹C. J. R. Counsell, J. W. Emsley, N. J. Heaton, and G. R. Luckhurst, *Mol. Phys.* **54**, 847 (1985).

¹⁰B. Janik, E. T. Samulski, and H. Toriumi, *J. Phys. Chem.* **91**, 1842 (1987).

¹¹C. J. R. Counsell, J. W. Emsley, G. R. Luckhurst, and H. S. Sachdev, *Mol. Phys.* **63**, 33 (1988).

¹²D. J. Photinos, E. T. Samulski, and H. Toriumi, *J. Phys. Chem.* **94**, 4688 (1990).

¹³D. J. Photinos, E. T. Samulski, and H. Toriumi, *J. Phys. Chem.* **94**, 4694 (1990).

¹⁴M. Gochin, A. Pines, M. E. Rosen, S. P. Rucker, and C. Schmidt, *Mol. Phys.* **69**, 671 (1990).

¹⁵D. J. Photinos, E. T. Samulski, and H. Toriumi, *Mol. Cryst. Liq. Cryst.* **204**, 161 (1991).

¹⁶A. Ferrarini, G. J. Moro, P. L. Nordio, and G. R. Luckhurst, *Mol. Phys.* **77**, 1 (1992).

¹⁷M. E. Rosen, S. P. Rucker, C. Schmidt, and A. Pines, *J. Phys. Chem.* **97**, 3858 (1993).

¹⁸G. Celebre and G. De Luca, *J. Phys. Chem. B* **107**, 3243 (2003).

¹⁹W. L. Meerts, C. A. de Lange, A. C. J. Weber, and E. E. Burnell, *J. Chem. Phys.* **130**, 044504 (2009).

²⁰A. C. J. Weber, A. Pizzirusso, L. Muccioli, C. Zannoni, W. L. Meerts, C. A. de Lange, and E. E. Burnell, *J. Chem. Phys.* **136**, 174506 (2012).

²¹A. Pizzirusso, M. E. Di Pietro, G. De Luca, G. Celebre, M. L. Muccioli, and C. Zannoni, *ChemPhysChem* **15**, 1356 (2014).

²²W. L. Meerts, C. A. de Lange, A. C. J. Weber, and E. E. Burnell, *Encyclopedia of Magnetic Resonance, Analysis of Complex High-Resolution NMR Spectra by Sophisticated Evolutionary Strategies* (John Wiley & Sons, Ltd., New York, 2013).

²³P. B. Woller and E. W. Garbisch, *J. Am. Chem. Soc.* **94**, 5310 (1972).

²⁴T. Tynkkynen, T. Hassinen, M. Tiainen, P. Soininen, and R. Laatikainen, *Magn. Reson. Chem.* **50**, 598 (2012).

²⁵E. E. Burnell, A. C. J. Weber, C. A. de Lange, W. L. Meerts, and R. Y. Dong, *J. Chem. Phys.* **135**, 234506 (2011).

²⁶A. C. J. Weber, R. Y. Dong, W. L. Meerts, X. Yang, and E. E. Burnell, *J. Phys. Chem. A* **117**, 9224 (2013).

²⁷A. C. J. Weber and D. H. J. Chen, *Mag. Reson. Chem.* **52**, 560 (2014).

²⁸W. L. Meerts and M. Schmitt, *Int. Rev. Phys. Chem.* **25**, 353 (2006).

²⁹A. C. J. Weber, X. Yang, R. Y. Dong, W. L. Meerts, and E. E. Burnell, *Chem. Phys. Lett.* **476**, 116 (2009).

³⁰Gaussian 09, Revision A.02, M. J. Frisch, G. W. Trucks, H. B. Schlegel, G. E. Scuseria, M. A. Robb, J. R. Cheeseman, G. Scalmani, V. Barone, B. Mennucci, G. A. Petersson, H. Nakatsuji, M. Caricato, X. Li, H. P. Hratchian, A. F. Izmaylov, J. Bloino, G. Zheng, J. L. Sonnenberg, M. Hada, M. Ehara, K. Toyota, R. Fukuda, J. Hasegawa, M. Ishida, T. Nakajima, Y. Honda, O. Kitao, H. Nakai, T. Vreven, J. A. Montgomery, Jr., J. E. Peralta, F. Ogliaro, M. Bearpark, J. J. Heyd, E. Brothers, K. N. Kudin, V. N. Staroverov, R. Kobayashi, J. Normand, K. Raghavachari, A. Rendell, J. C. Burant, S. S. Iyengar, J. Tomasi, M. Cossi, N. Rega, J. M. Millam, M. Klene, J. E. Knox, J. B. Cross, V. Bakken, C. Adamo, J. Jaramillo, R. Gomperts, R. E. Stratmann, O. Yazyev, A. J. Austin, R. Cammi, C. Pomelli, J. W. Ochterski, R. L. Martin, K. Morokuma, V. G. Zakrzewski, G. A. Voth, P. Salvador, J. J. Dannenberg, S. Dapprich, A. D. Daniels, O. Farkas, J. B. Foresman, J. V. Ortiz, J. Cioslowski, and D. J. Fox, Gaussian, Inc., Wallingford CT, 2009.

³¹C. Möller and M. S. Plesset, *Phys. Rev.* **46**, 618 (1934).

³²T. H. Dunning, *J. Chem. Phys.* **90**, 1007 (1989).

³³J. B. Klauda, B. R. Brooks, A. D. MacKerell, R. M. Venable, and R. W. Pastor, *J. Phys. Chem. B* **109**, 5300 (2005).

³⁴A. C. J. Weber, C. A. de Lange, W. L. Meerts, and E. E. Burnell, *Chem. Phys. Lett.* **496**, 257 (2010).

³⁵A. C. J. Weber and E. E. Burnell, *Chem. Phys. Lett.* **506**, 196 (2011).

³⁶E. B. Wilson, Jr., J. C. Decius, and P. C. Cross, *Molecular Vibrations, The Theory of Infrared and Raman Vibrational Spectra* (Dover, New York, 1955).

- ³⁷N. J. D. Lucas, *Mol. Phys.* **22**, 147 (1971).
- ³⁸N. J. D. Lucas, *Mol. Phys.* **22**, 233 (1971).
- ³⁹N. J. D. Lucas, *Mol. Phys.* **23**, 825 (1972).
- ⁴⁰J. G. Snijders, C. A. de Lange, and E. E. Burnell, *Isr. J. Chem.* **23**, 269 (1983).
- ⁴¹J. Lounila and P. Diehl, *J. Magn. Reson.* **56**, 254 (1984).
- ⁴²J. Lounila and P. Diehl, *Mol. Phys.* **52**, 827 (1984).
- ⁴³A. Loewenstein and M. Brenman, *Chem. Phys. Lett.* **58**, 435 (1978).
- ⁴⁴C. A. de Lange, W. L. Meerts, A. C. J. Weber, and E. E. Burnell, *J. Phys. Chem. A* **114**, 5878 (2010).
- ⁴⁵W. Maier and A. Saupe, *Z. Naturforsch. A* **14**, 882 (1959).
- ⁴⁶W. Maier and A. Saupe, *Z. Naturforsch. A* **15**, 287 (1960).